The Energy Management Control System of the DC Microgrid Based on the Three-Step Approach for Office Buildings

Hui Qiao and Kusumal Chalermyanont
Department of Electrical Engineering, Prince of Songkla University, Songkhla, Thailand

Abstract

This paper proposes an energy management control system (EMCS) to manage and optimize power in dc microgrid system. The system consists of PV, AC grid and energy storage to supply the dc loads in the office building. The dc microgrid system and the EMCS module are built based on the MATLAB/Simulink platform. The suitable constraints such as the limit value of SOC of the system for the next day's condition are obtained by considering from the day ahead predicted values of PV power and load demand. Based on those constraints, power supply priority of system sources and real-time operation algorithm, the real time control signals of PV, AC grid and the battery are performed to control and optimize the system energy and reduce supplying time of AC grid. The PV is controlled between maximum power point tracking (MPPT) and load demand power point tracking (LPPT) algorithms due to the limitations of the energy storage system.

Keywords : dc microgrid, dc bus voltage, energy management control system (EMCS), load power point tracking (LPPT), real-time operation algorithm, variable dc load.

I. Introduction

Until now, the main energy supply of office buildings is still the AC Power Grid. The characteristics of high power demand in the daytime and low power demand at night for the load of the office building are similar to the power supply characteristics of PV. However, the output power of PV is depending on weather conditions (temperature and irradiance), which is unstable, therefore, the use of the energy storage system is necessary.

As a module to improve the performance of the electrical power system, the energy management control system has become an indispensable part of the microgrid system. There are three main performance considerations. [1] and [2] using a load shedding approach to reduce system cost. In [3], a multi-objective optimization is used to reduce system generating cost. The above three papers use an energy management system to improve the economy of the microgrid system. In [4], the local drivers are used to optimal switching frequency, which achieves the microgrid system voltage stability. In [5], the optimal power dispatching method is used to reduce the electrical charge and increase the peak-to-average ratio of the microgrid system. Autonomous control strategies are used for the islanded microgrid, which autonomously matches the varying load and makes the system power balance [6]. In [7], a robust optimal power management system is proposed to satisfy the load demand with maximum utilization of renewable resources. The above four papers mainly improve the stability of the microgrid system through an energy management system. In [8] and [9], the maximum power point tracking algorithm is

used for renewable energy to maximize energy generation. Two operation mode of energy storage scheduling is used to the minimal investment cost and enhance system energy [10]. The above three papers mainly improve the efficiency of the microgrid system by using an energy management system.

Compared with previous papers on the energy management system, this paper also realizes the economy, stability and high efficiency of the system through an energy management control system. The difference is in the way they are implemented.In this paper,the use of MPPT achieves the efficient production capacity of renewable energy. The priority of the microgrid system sources is set to reduce the energy consumption of AC utility grid. The use of LPPT reduces the charge and discharge energy of the battery. What' more, by combining the real-time operation algorithm, the power stability of the system is improved. In particular, the flexibility of microgrid systems is improved by setting constraints on the state of charge of the battery based on different weather conditions.

II. Research Methodology

A. Load Forecasting Method

Neural Network autoregression (NNAR) [11] have a strong learning ability that weights and bias are trained based on errors until the error reduced to the acceptable range. In this paper, using feed-forward networks to forecast load demand.

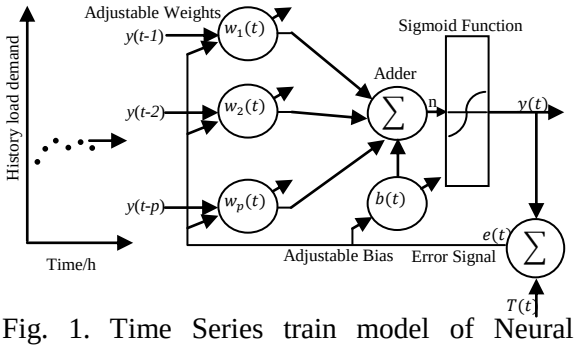

Fig. 1. Time Series train model of Neural Network autoregression

For time series load demand data, using the notation $NNAR(p,P,k)_m$ to indicate there are p lagged inputs and k nodes in the hidden layer. If k is not specified, it is set to $k=(p+P+1)/2$ (rounded to the nearest integer), and with the seasonal data, adding the last observed values from the same season as inputs. For example, $NNAR(p,P,k)_m$ model has inputs $(y_{t-1},\ y_{t-2},\ \cdots,\ y_{t-p},\ y_{t-m},\ y_{t-2m},\ y_{t-Pm})$ and k hidden layers. The train model of NNAR is shown as Fig. 1.

When it comes to forecasting, the network is applied iteratively. For forecasting one step, simply using the available historical inputs. For forecasting two steps, using the one-step forecast as an input, along with the historical data.

B. Load demand Power Point Tracking

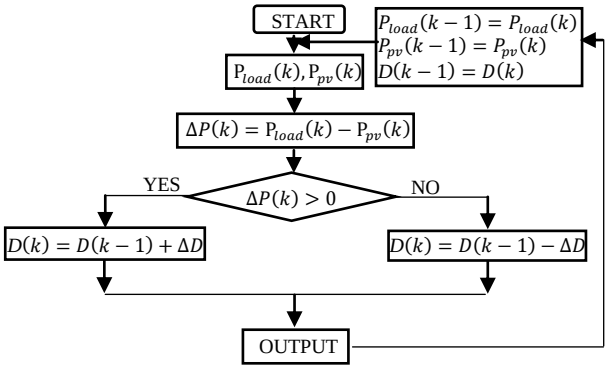

Fig. 2. Load demand power point tracking flow chart

LPPT algorithm is shown as Fig. 2. Where $k=10^{-6}$, is the sample time, and $\Delta D=5\times10^{-6}$, which is the perturbation value, additionally, D is the duty cycle of PV. Besides, P_{load} and P_{pv} are the real time load demand and real time active power of PV respectively.

III. Proposed EMCS

Each component of DC microgrid and proposed EMCS architecture are shown in Fig. 3 and Fig. 4.

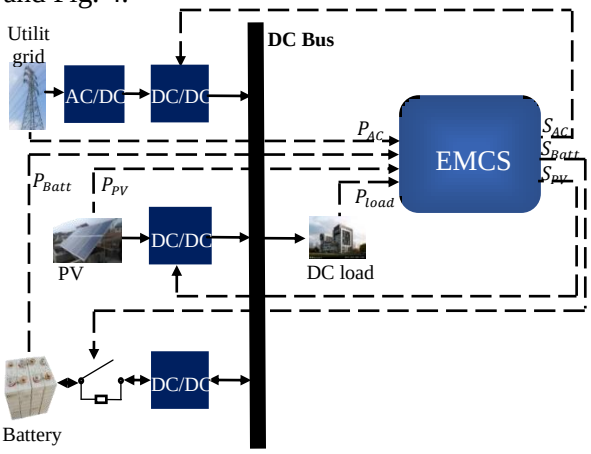

Fig. 3. DC microgrid real-time control architecture

In this system, as the main power supply equipment, PV is used to provide energy for the DC load. Besides, the battery as the energy storage equipment and the AC power grid as the backup energy jointly maintains the stability of the system.

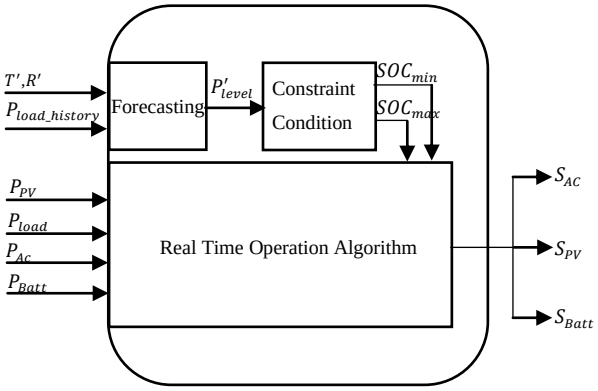

Fig. 4. Energy Management Control System architecture

The EMCS includes three steps: forecasting, constraint condition, and real-time operation algorithm. Based on the constraints of the battery obtained from the first and second steps (SOC_{min}, SOC_{max}) and the real-time power value of each components of the system (P_{PV}, P_{load}, P_{Ac}, P_{Batt}), the control signal of PV (S_{PV}), AC grid (S_{AC}), and battery (S_{Batt}) be given by the EMCS.

A. Forecasting

In this paper, PV power and load demand forecasting for the next day are included in the first step of the EMCS, the day ahead forecasting of power and load demand are shown as follows:

1). Day-ahead load demand forecasting based on NNAR method.

The history load demand collected from the total electricity load demand of Germany in 2015 of the pan-European market of the entsoe Transparency Platform is used as the time series research data. Moreover, NNAR is a suitable method to predict seasonal time series load demand. The next day load demand (P'_{load}) is forecasted based on the history load demand data ($P_{load\_history}$).

2). Day-ahead PV power forecasting based on PV model.

PV Simulink model is used for PV power forecasting. Since the simulation model of PV has been established, if the predicted value of the inputs (T', R') can be acquired, the predicted value of maximum PV power (P'_{PV_max}) can be obtained through the characteristic curve of this model. In this paper, the forecasting value of temperature and Irradiation can be got from Meteorological website.

B. Constraint Condition

Based on forecasting value of PV power and load demand, the maximum overflow of energy (P'_{level_O}) and the maximum shortage of energy (P'_{level_S}) are got, which can decide the limits of Battery (SOC_{max}, and SOC_{min}). The battery parameters limiting process is shown as Fig. 5.

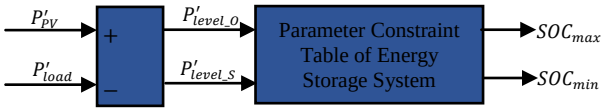

Fig. 5. The battery parameters limiting process

The equation of P'_{level_O} and P'_{level_S} are shown as (1) and (2) respectively.

when $P'_{PV} \gg P'_{load}$

$$P'_{level\_O} = max\{P'_{PV}(i) - P'_{load}(i)\} \quad (1)$$

when $P'_{PV} < P'_{load}$

$$P'_{level\_S} = max|P'_{PV}(i) - P'_{load}(i)| \quad (2)$$

Where $i = 1, 2, \ldots, 24$ is the sample point. P'_{PV} and P'_{load} are the forecasting power of PV and forecasting load demand respectively. The constraint values of the parameter as shown in Table I.

Table I. Constraint Parameters of Energy Storage System

P'_{level_O}/W	$SOC_{max}/\%$	P'_{level_S}/W	$SOC_{min}/\%$
12000-30000	65	0-55000	45
5000-12000	60	55000-65000	40
0-5000	55	65000-70000	35

It is well known that the service life of lithium batteries is related to the maximum depth of discharge (MDOD) [12]. The deeper the MDOD, the shorter the service life of lithium battery. However, the MDOD is too shallow to meet the demand of the microgrid system. Combined with the maximum historical energy shortage value and the battery capacity, in this paper, the MDOD is selected in the range of 55%-65%, and the SOC_{max} and SOC_{min} are

divided into three levels according to the values of P'_{level_O} and P'_{level_S} respectively.

Because the weather affects the PV power generation, thus affecting the value of P'_{level_O} and P'_{level_S}. Therefore, choosing the limitation of SOC of the battery according to different weather conditions can make the dc microgrid more adaptable.

C. Real-Time Operation Algorithm

Based on the limit values of the battery obtained in the second step, the real-time operation strategy is used to control and optimize the energy flow of the DC micro-grid system and show in Fig. 6.

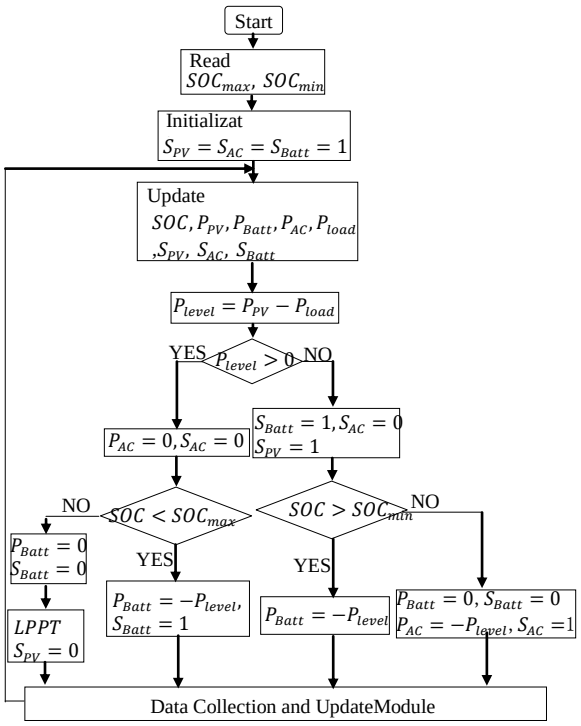

Fig. 6. The real-time operation algorithm

The control strategy considers two aspects. First one is when the PV power is less than the load demand ($P_{level} \leq 0$). The MPPT algorithm can be used the PV (S_{PV}=1), and the insufficient energy is supplied from the battery (S_{Batt}=1). It's worth mentioning that the AC grid as a backup device, use only when the battery is unable to supply the load demand (When the AC grid provides power, S_{AC}=1). The second one, PV power is higher than the load demand ($P_{level} > 0$), and after the state of charge of the battery reaches to SOC_{max}. In order to reduce the battery charge and discharge energy and make the system energy balance, the PV array runs under the LPPT ($S_{PV} = 0$, S_{Batt}=0, and S_{AC}=0).

IV. Experiment Result and Analysis

A. The Result of Load Demand Forecast and PV Energy Forecast

The training and testing data using NNAR method are shown in Fig. 7 in time series. In addition, the result of forecasting load demand and the actual load demand in 30^{th} January 2015 is shown in Fig. 8 (The main purpose of this paper is to verify the feasibility of the established EMCS, and because the obtained load demand is too large, the value of the load demand used in this paper is the collected load demand value divided by a trillion). The raw data is sampled every hour from 5^{th} January 2015 – 30^{th} January 2015. In order to improve the accuracy of prediction, this paper choose similar day as history data to forecasting day ahead load demand (load demand data of Fri. Jan. 9^{th}, 2015, Fri. Jan. 16^{th}, 2015 and Fri. Jan. 23^{rd}, 2015 is used as the historical data to forecasting load demand data of Fri. Jan. 30^{th} 2015).

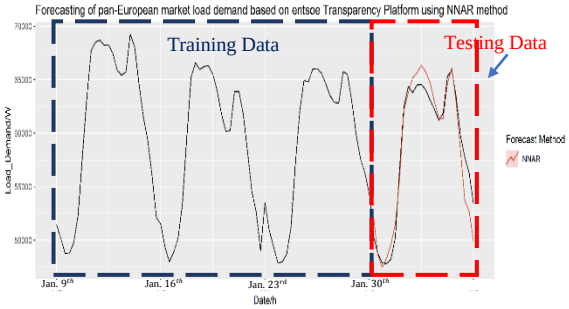

Fig. 7. The prediction results containing the training and testing data using NNAR method

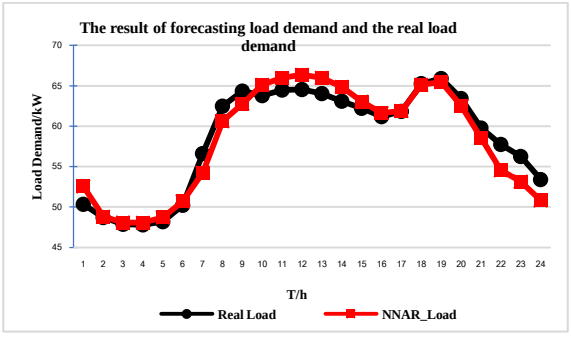

Fig. 8. The result of forecasting load demand and the actual load demand in 30^{th} January 2015

The predicted irradiation is shown as Fig. 9. The predicted temperature is 25 ℃ (Since weather data corresponding to cities with load

demand cannot be obtained, the predicted values of irradiation and temperature used in this paper are simplified and adjusted based on real data (other cities) in order to verify the performance of EMCS). PV array energy prediction is based on MATLAB/Simulink PV model. Since a PV simulation model has been established in MATLAB/Simulink, if the predicted and actual values of the PV model inputs (irradiation and temperature) can be obtained, the predicted and actual values of the PV energy can be obtained. Fig. 10 shows the forecasting maximum power of PV based on the forecasting weather condition. In this paper, there are Simulink time 7.2 seconds, and 24 simulation sampling points, it simulates a full day (24 hours) of real time.

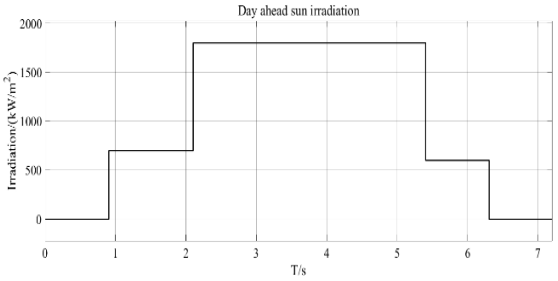

Fig. 9. Day ahead forecasting irradiance

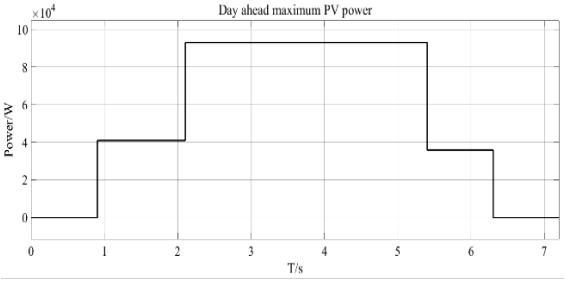

Fig. 10. Day ahead forecasting maximum power of PV

B. Results of Restriction

Based on the constraint parameters in the table of the energy storage system, the restriction of the battery, in this case, is specified in Table II.

Table II. The result of the restriction of battery

P'_{level_0}/W	SOC_{max}/%	P'_{level_S}	SOC_{min}/%
10000	60	56265	40

C. Simulink Results of The Real-Time Operation

The result of the output control signal of EMCS is shown as Fig. 11. When the $S_{Batt} = 1$ and $S_{AC} = 1$ the Battery and AC grid can exchange power with DC microgrid, otherwise, both of them can't exchange power with the system. Additionally, when the $S_{PV} = 1$, the PV performs in MPPT algorithm, otherwise, it will operate in LPPT algorithm.

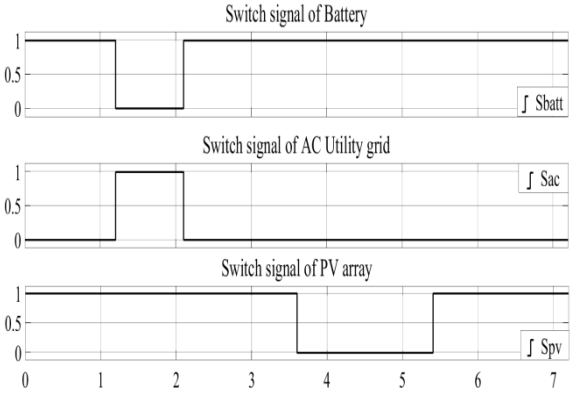

Fig. 11. The Control Signal of Simulink result of EMCS

The simulation results of the energy of each part of the DC microgrid system obtained without the EMCS are shown in Fig. 12. As can be seen from the figure, when PV power is insufficient to meet the load demand, at the same time, the battery and AC utility grid provide power for the DC microgrid system. AC utility grid keeps supplying electricity until PV power exceeds the load demand. In this case, AC supply more energy to the DC microgrid system. Moreover, when PV power is higher than the load demand, the battery will continue to be charged until PV power is lower than the load demand again.

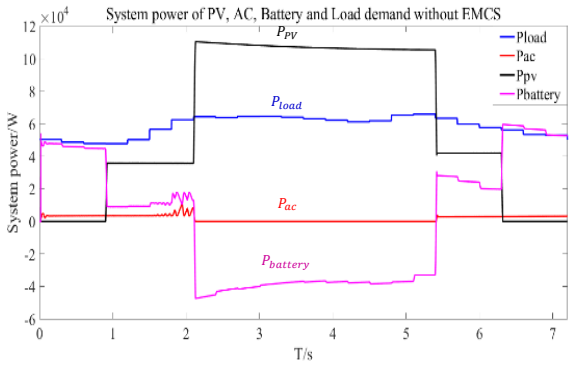

Fig. 12. Simulink result of the power of DC microgrid System without EMCS

Based on the battery restriction of the energy storage system obtained in the second step of the EMCS, and combined with the real-time control algorithm in the third step, the simulation results of the energy of each part of the DC microgrid system under actual weather conditions are shown in Fig. 13.

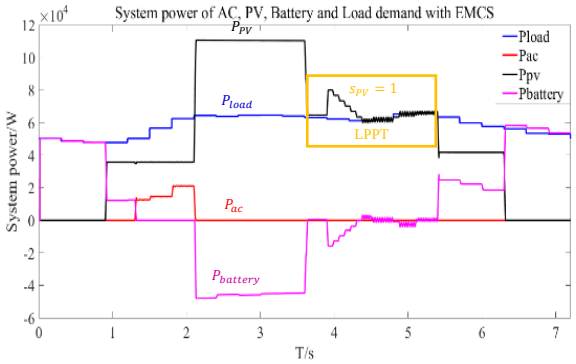

Fig. 13. Simulink result of the power of DC microgrid system with EMCS

When PV power is lower than the load demand, batteries provide power to the system in priority. This is because the power supply priority of battery, AC utility grid and PV array is set from high to low, which can reduce the consumption of AC energy fossil energy. However, when the simulation time is 1.2 seconds, the PV power is still lower than the load demand, the battery is no longer powering the system which is because of the limit parameter of the SOC of the battery, in this time period, ac utility grid supply for the system. When the time is 1.2 seconds, the SOC of the battery below the level of SOC_{min} (40%). When the simulation time is 2.1 seconds, the battery is charging, because of the SOC of the battery not up to the limit. At this time, the AC utility grid no longer provides energy. When the Simulink time is 3.6 seconds, the PV power tracking the load demand and the battery charging and discharging energy is close to zero. The reason for this result is that PV uses LPPT algorithm.

In comparison, the dc microgrid system with EMCS shows better characteristics

To identify the performance of the EMCS, the energy of battery and AC are quantitatively calculated within a day and compare to the case without the EMCS. The comparison results are shown in Table III.

Table III. The energy between AC and battery

Situation \ Energy	The Energy of AC (kW · h)	The Energy of charge and discharge of Battery (kW · h)
Without EMCS	60	877
With EMCS	45	603

From Table III can be seen that with the addition of the EMCS, the charge and discharge energy of battery significantly reduced compared with no EMCS, which reduces maintenance frequency and conducive to extending the battery lifetime. Besides, the energy consumption of AC utility decreased significantly, which reduces the system costs.

V. Conclusion

In this paper, the adjustment of the limit of battery parameters based on the predicted value of PV power and load demand enables the system to adapt to different weather conditions and improves the flexibility of the DC microgrid system. Combined with the limitation of the battery and the LPPT algorithm, the battery charge and discharge energy are reduced significantly, which reduces the frequency of maintenance and extends the lifetime of the battery. What's more, by setting the power supply priority, the energy consumption of the AC utility grid is reduced. Moreover, the energy flow of each component of the DC microgrid can run according to the real-time operation strategy of the EMCS and maintain the power balance.

References

[1] L. Trigueiro dos Santos, M. Sechilariu, and F. Locment, "Optimized Load Shedding Approach for Grid-Connected DC Microgrid Systems under Realistic Constraints," Buildings, vol. 6, no. 4, p. 50, Dec. 2016.

[2] S. Koohi-Kamali and N. A. Rahim, "Coordinated control of smart microgrid during and after islanding operation to prevent under frequency load shedding using energy storage system," Energy Conversion and Management, vol. 127, pp. 623–646, Nov. 2016.

[3] X. Lu, Y. Chen, M. Fu, and H. Wang, "Multi-Objective Optimization-Based Real-Time Control Strategy for Battery/Ultracapacitor Hybrid Energy Management Systems," IEEE Access, vol. 7, pp. 11640–11650, 2019.

[4] García Elvira, H. Valderrama Blaví, À. Cid Pastor, and L. Martínez Salamero, "Efficiency Optimization of a Variable Bus Voltage DC Microgrid," Energies, vol. 11, no. 11, p. 3090, Nov. 2018.

[5] H. Sharifi and P. Maghouli, "Energy management of smart homes equipped with energy storage systems considering the PAR index based on real-time pricing," Sustainable Cities and Society, vol. 45, pp. 579–587, Feb. 2019.

[6] H. Mahmood, D. Michaelson, and J. Jiang, "Strategies for Independent Deployment and Autonomous Control of PV and Battery Units in Islanded Microgrids," IEEE Journal of Emerging and Selected Topics in Power Electronics, vol. 3, no. 3, pp. 742–755, Sep. 2015.

[7] M. Hosseinzadeh and F. R. Salmasi, "Robust Optimal Power Management System for a Hybrid AC/DC Micro-Grid," IEEE Transactions on Sustainable Energy, vol. 6, no. 3, pp. 675–687, Jul. 2015.

[8] N. Eghtedarpour and E. Farjah, "Control strategy for distributed integration of photovoltaic and energy storage systems in DC micro-grids," Renewable Energy, vol. 45, pp. 96–110, Sep. 2012.

[9] M. Gunasekaran, H. Mohamed Ismail, B. Chokkalingam, L. Mihet-Popa, and S. Padmanaban, "Energy Management Strategy for Rural Communities' DC Micro Grid Power System Structure with Maximum Penetration of Renewable Energy Sources," Applied Sciences, vol. 8, no. 4, p. 585, Apr. 2018.

[10] W. S. Ho, S. Macchietto, J. S. Lim, H. Hashim, Z. A. Muis, and W. H. Liu, "Optimal scheduling of energy storage for renewable energy distributed energy generation system," Renewable and Sustainable Energy Reviews, vol. 58, pp. 1100–1107, May 2016.

[11] Rob J. Hyndman and George Athanasopoulos, "Forecasting: Principles and Practice," OTexts, May. 8, 2018, Monash University, Australia. [Online]. Available: https://otexts.org/fpp2/.

[12] S. Cheng, Y.-H. Liu, H. Hesse, M. Naumann, C. Truong, and A. Jossen, "A PSO-Optimized Fuzzy Logic Control-Based Charging Method for Individual Household Battery Storage Systems within a Community," Energies, vol. 11, p. 469, Feb. 2018.